

# Mercury Stable Isotopic Compositions in Coals from Major Coal Producing Fields in China and Their Geochemical and Environmental Implications

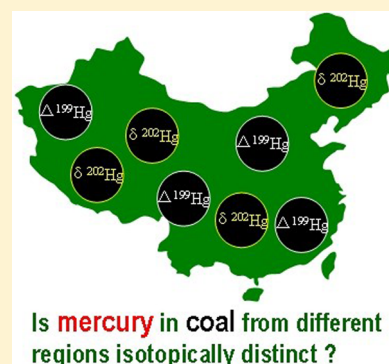
Runsheng Yin,<sup>†,‡</sup> Xinbin Feng,<sup>\*,†</sup> and Jiubin Chen<sup>†</sup>

<sup>†</sup>State Key Laboratory of Environmental Geochemistry, Institute of Geochemistry, Chinese Academy of Sciences, Guiyang 550002, China

<sup>‡</sup>State Key Laboratory of Ore Deposit Geochemistry, Institute of Geochemistry, Chinese Academy of Sciences, Guiyang, 550002, China

## S Supporting Information

**ABSTRACT:** Total mercury (Hg) concentrations (THg) and stable mercury isotopic compositions were measured in coal samples ( $n = 61$ ) from major coal producing fields in China. The THg concentrations in coals ranged from 0.05 to 0.78  $\mu\text{g g}^{-1}$ , with a geometric mean of 0.22  $\mu\text{g g}^{-1}$ . Hg isotopic compositions in coals showed large variations both in mass-dependent fractionation (MDF,  $\delta^{202}\text{Hg}$ :  $-2.36$  to  $-0.14\text{‰}$ ) and mass-independent fractionation (MIF,  $\Delta^{199}\text{Hg}$ :  $-0.44$  to  $+0.38\text{‰}$ ). The MIF signatures in coals may reveal important information on the coal-forming conditions (e.g., humic and sapropelic). The  $\Delta^{199}\text{Hg}/\Delta^{201}\text{Hg}$  of  $\sim 1$  determined in coals indicated that a portion of Hg has been subjected to photoreduction process prior to being incorporated to coals. On the basis of THg, Hg isotopic signatures, and other geological factors (e.g., total ash content and total sulfur content), the potential sources of Hg in coals from different coal producing regions were estimated. The main source of Hg in coals from southwestern China and eastern part of northern China is likely geogenic Hg, whereas the source of Hg in coals from other parts of northern China is mainly biogenic Hg. Finally, we estimated that Hg emission from coal combustion in China is characterized by diagnostic Hg isotopic signatures ( $\delta^{202}\text{Hg}$ :  $\sim -0.70\text{‰}$  and  $\Delta^{199}\text{Hg}$ :  $\sim -0.05\text{‰}$ ). The present study demonstrates that Hg isotopes can serve as a tool in understanding the sources and transformation of Hg in coals and may also be used as a tracer to quantify Hg emissions from coal combustion.



## INTRODUCTION

Mercury (Hg) is known as a global pollutant due to its long-range transport and persistence in the environment.<sup>1</sup> Hg is naturally present in coal and is emitted to the air when coal is burnt as fuel. Coal combustion has been demonstrated to be the largest anthropogenic source of Hg emissions to the atmosphere.<sup>2</sup> China is currently the largest producer and consumer of coal in the world. Total Hg emissions from China have increased rapidly in recent years.<sup>2</sup> Evaluation of Hg emissions from coal combustion in China has been studied with indirect measurements of Hg abundance and mathematical modeling.<sup>3,4</sup> However, the large uncertainty in Hg content in coal and the paucity of information on Hg emission factors during coal combustion processes limited our understanding on the environmental impacts of this major anthropogenic Hg source.<sup>4</sup> Consequently, new approaches are thus needed to trace and quantify the environmental impact of Hg emissions from Chinese coals both on regional and global scales.

During past decade, multiple-collector inductively coupled plasma mass spectrometry (MC-ICP-MS) and associated sample preparation techniques have been largely improved, which allow for high-precision measurements of Hg isotopes in environmental samples.<sup>5,6</sup> Hg has seven stable isotopes ( $^{196}\text{Hg}$ ,

$^{198}\text{Hg}$ ,  $^{199}\text{Hg}$ ,  $^{200}\text{Hg}$ ,  $^{201}\text{Hg}$ ,  $^{202}\text{Hg}$  and  $^{204}\text{Hg}$ ). Previous studies reported significant Hg isotope variations in Hg ores,<sup>7–10</sup> hydrothermal emissions,<sup>11,12</sup> sediments/soils,<sup>13–17</sup> coal,<sup>18–21</sup> and fishes.<sup>5,22</sup> Hg isotopes can be systematically fractionated during microbiological reduction,<sup>23,24</sup> methylation,<sup>25</sup> demethylation,<sup>26</sup> photoreduction,<sup>5,27</sup> volatilization,<sup>28</sup> evaporation,<sup>29</sup> and adsorption.<sup>30</sup> In addition to mass-dependent fractionation (MDF), mass-independent fractionation (MIF) of both the even and odd Hg isotopes also takes place, which provides additional information on tracing sources and fates of Hg in the environment.<sup>5,31–34</sup>

The Hg isotopic compositions of coals have been previously investigated.<sup>18–21</sup> Biswas et al.<sup>18</sup> observed a 3‰ range in  $\delta^{202}\text{Hg}$  and a 1‰ range in  $\Delta^{199}\text{Hg}$  for coal samples collected from the U.S., China, Russia, and Kazakhstan. Their study suggested that the combination of MDF and MIF signatures of Hg isotopes could be employed as a diagnostic tool for “fingerprinting” anthropogenic Hg from different coal sources.

**Received:** January 21, 2014

**Revised:** April 15, 2014

**Accepted:** April 17, 2014

**Published:** April 17, 2014

Lefticariu et al.<sup>19</sup> investigated the Hg isotopic compositions of coal samples from four coal deposits (Illinois Basin, U.S.). They suggested that syngenetic and epigenetic Hg sources in coal have distinct Hg isotope signatures.<sup>19</sup> Sun et al.<sup>21</sup> investigated the potential Hg isotope fractionation in six utility boilers of two large Chinese coal fired power plants. Sherman et al.<sup>20</sup> used the Hg isotopes as a fingerprint to track Hg emissions from a power plant in Florida, USA. Biswas et al.<sup>18</sup> reported Hg isotopic compositions in 11 Chinese coal samples and demonstrated large variations of both MDF ( $\delta^{202}\text{Hg}$ :  $-2.70$  to  $-0.28\text{‰}$ ) and MIF ( $\Delta^{199}\text{Hg}$ :  $-0.44$  to  $+0.38\text{‰}$ ). Even though these samples may not represent the overall Hg isotopic compositions of Chinese coal due to limited number of coal samples collected, it implies that coal from different coal producing regions may have different Hg isotopic compositions. To better understand the geochemical constraints and the environmental impacts of Hg in Chinese coals, measurements of Hg concentrations and Hg isotopic compositions in coals collected from the main coal producing regions of China were made. The objectives of the study are (1) to identify possible sources of Hg in coals and (2) to characterize the isotopic signature of Hg emitted from coal combustion in China.

## ■ EXPERIMENTAL SECTION

**Main Coal Producing Regions in China and the Sampling Sites.** Figure S1 (Supporting Information) shows the sampling sites of 61 coals in 18 provinces in China. As shown in Figure S1 (Supporting Information), based on the resource distribution and the yield of coal production as well as the consideration of ranking by coal type and coal-forming periods,<sup>36</sup> five main coal producing regions can be identified in China. These are (1) the Late Jurassic ( $J_3$ ) coal producing region in northeastern China, (2) the Permo-carboniferous ( $C-P$ ) coal producing region in northern China, (3) the Late Permian ( $P_2$ ) coal producing region in southern China, (4) the Early-Middle Jurassic ( $J_{1-2}$ ) coal producing region in northwestern China, and (5) the Mesozoic–Cenozoic ( $M-C$ ) coal producing region in Yunnan Province and Tibet. Since the Hg concentrations in coals from  $J_{1-2}$  and  $J_3$  are too low for Hg isotope analysis (see Result and Discussion), only a few coal samples were collected from these regions. The  $M-C$  coal producing region has not been extensively exploited because the coal reserves in this region only account for <1% of the total coal resources in China,<sup>36</sup> and therefore, no coal samples were collected in this region. Samples were collected by a channel sampling method according to the State Bureau of Technical Supervision (SBTS).<sup>35</sup> Briefly, in each sampling site, the weathered surface of the coal exposure was first removed, and the fresh face of the coal bed was evened. Then, a channel sample (approximately 15 cm in diameter and 5 cm deep) was taken from an integrated profile of each coal bed. Each collected sample was further divided into at least 5 subsamples, and a 5 kg sample was selected for analysis. Detailed information for the collected coal samples is given in Table S1 (Supporting Information).

**Total Hg Concentration Analysis.** The THg concentrations in coal samples were first determined by a combustion method using Lumex RA 915+ Hg analyzer.<sup>37</sup> The quality assurance (QA) and quality control (QC) of our analysis was assessed using the certified reference material (NIST SRM 2711, Montana soil), with the recovery ranging from 91 to 101% (Mean:  $96 \pm 7\%$ ,  $2\sigma$ ,  $n = 6$ ). We also used a wet

digestion method to determine THg concentrations in coal. Approximately 0.5 g of coal sample was weighed into a 50 mL Teflon bomb digester. Then, 18 mL of oxidizing acid, which contains 15 mL of aqua regia ( $\text{HNO}_3/\text{HCl} = 3/1$ ) and 3 mL of HF, was slowly added to avoid violent reaction. Teflon bomb digesters were screw tightened and were heated on a hot plate at  $110\text{ }^\circ\text{C}$  for 24 h. The digested solutions were centrifuged (3500 rpm, 15 min) to separate the residues and were evaporated ( $120\text{ }^\circ\text{C}$ ) to distill excessive acid until 5 mL concentrated solutions were gained. Finally, all solutions were diluted to 25 mL for THg analysis. All the coal samples were prepared in duplicate ( $n = 2$ ). Ultrapure grade acid ( $\text{HNO}_3$  and  $\text{HCl}$ ) and Mill-Q water ( $18.2\text{ M}\Omega\text{ cm}$ ) were used. THg concentrations in coal digests were also determined by cold vapor atomic fluorescence spectrometry (Tekran 2500, Canada),<sup>38</sup> which agreed well with the THg data measured by the combustion method (Table S1, Supporting Information). The analytical blanks were  $<29\text{ pg mL}^{-1}$ . The average THg recovery of NIST SRM 2711 using the wet digestion method ranged from 86 to 96%. The average recovery for wet digestion method ( $93 \pm 8\%$ ,  $2\sigma$ ,  $n = 6$ ) was comparable with the combustion method ( $96 \pm 7\%$ ,  $2\sigma$ ,  $n = 6$ ), which validates our wet digestion method. To evaluate the recovery of Hg during the sample preparation, the standard-addition method was also used. Various amounts (0–500 ng) of NIST SRM 3133 Hg standard were treated using the complete sample digestion protocol as described above. The measured Hg and the added Hg defined a straight line ( $n = 8$ ,  $r^2 = 0.99$ ) (Figure S2, Supporting Information) suggested no loss of Hg during the sample digestion process.

**Coal rank, Total Sulfur Content, and Total Ash Content Determination.** The total sulfur concentration ( $C_s$ ) in coal samples was determined according to the American Society for Testing and Materials (ASTM) method.<sup>39</sup> Approximately 0.25 g of coal sample was weighed in a ceramic combustion boat, and burnt at  $\sim 1350\text{ }^\circ\text{C}$  in a stream of high purity oxygen gas to oxidize the sulfur. The sulfur dioxides ( $\text{SO}_2$ ) were released and their contents were measured by the sulfur analyzer (LECOR SC132). The ash content ( $C_A$ ) of coal samples was determined by weighing the residue remaining after burning a coal sample under rigidly controlled conditions according to the ASTM method.<sup>40</sup> The coal ranks of the samples were classified according to the ASTM method.<sup>41</sup>

**Hg Isotopic Composition Analysis.** On the basis of THg analysis, most of digested solutions were diluted to  $2\text{--}5\text{ ng mL}^{-1}$  prior to Hg isotope analysis. For coals with  $\text{THg} < 0.10\text{ }\mu\text{g g}^{-1}$ , digested solutions were diluted to  $1\text{ ng mL}^{-1}$ . The acid concentrations of the diluted solutions were  $<20\%$ . Hg isotopic compositions were determined by Nu-Plasma MC-ICP-MS using a previously established method.<sup>42</sup> Hg isotopic compositions are reported in terms of per mil deviations from NIST SRM 3133 Hg standard and expressed in “delta” ( $\delta$ ) notation (proposed by Blum and Bergquist<sup>43</sup>):

$$\delta^{\text{xxx}}\text{Hg}(\text{‰}) = \left\{ \left( \frac{{}^{\text{xxx}}\text{Hg}}{{}^{198}\text{Hg}}_{\text{sample}} \right) / \left( \frac{{}^{\text{xxx}}\text{Hg}}{{}^{198}\text{Hg}}_{\text{NISTSRM3133}} \right) - 1 \right\} \times 1000 \quad (1)$$

where xxx is mass of each Hg isotope between 199 and 202 amu. MIF is reported in capital delta notation ( $\Delta^{\text{xxx}}\text{Hg}$ , deviation from mass dependency in units of permil, ‰) using the following formulas:<sup>43</sup>

Table 1. Hg Concentration and Hg Isotopic Composition in Different Coal Ranks

regions	coal rank	geological age	geometric mean THg ( $\mu\text{g g}^{-1}$ )	$\delta^{202}\text{Hg} \text{‰}$	$2\sigma \text{‰}$	$\Delta^{199}\text{Hg} \text{‰}$	$2\sigma \text{‰}$	$\Delta^{201}\text{Hg} \text{‰}$	$2\sigma \text{‰}$	N
SW China	sub-bituminous	Permian	0.42	−0.93	0.10	−0.04	0.04	0.03	0.04	2
	bituminous	Permian	0.36	−0.85	0.76	−0.03	0.09	−0.05	0.06	12
		Triassic	0.32	−1.53	0.10	−0.08	0.06	0.02	0.10	1
eastern part of Northern China	anthracite	Permian	0.41	−0.59	1.16	−0.01	0.11	−0.03	0.16	2
	bituminous	Carboniferous	0.23	−0.74	1.05	−0.01	0.11	−0.02	0.10	5
		Permian	0.24	−0.79	0.33	−0.04	0.17	−0.05	0.15	9
		Carboniferous	0.29	−0.26	0.20	−0.05	0.04	−0.07	0.06	1
		Permian	0.41	−0.71	0.68	0.06	0.13	0.02	0.14	2
other parts of China	lignite	Jurassic	0.07	−1.13	0.30	0.15	0.08	0.11	0.06	1
		Carboniferous	0.11	−1.00	0.62	−0.10	0.18	−0.16	0.22	1
	bituminous	Permian	0.3	−0.65	0.22	−0.10	0.02	−0.14	0.10	1
		Jurassic	0.08	−0.76	0.30	−0.27	0.27	−0.23	0.24	2
		Carboniferous	0.20	−0.95	1.16	−0.02	0.07	−0.03	0.11	6
		Permian	0.15	−1.66	0.71	−0.06	0.53	−0.05	0.54	6
		Jurassic	0.08	−0.98	0.76	−0.26	0.23	−0.24	0.19	4
		Carboniferous	0.19	−1.04	0.92	−0.04	0.07	0.00	0.11	2
	anthracite	Carboniferous	0.19	−1.04	0.92	−0.04	0.07	0.00	0.11	2
		Permian	0.15	−1.52	1.66	−0.16	0.55	−0.14	0.47	4

Table 2. Hg Concentration and Hg Isotopic Composition in Different Coal Forming Periods

regions	geological age	coal rank	geometric mean THg ( $\mu\text{g g}^{-1}$ )	$\delta^{202}\text{Hg} \text{‰}$	$2\sigma \text{‰}$	$\Delta^{199}\text{Hg} \text{‰}$	$2\sigma \text{‰}$	$\Delta^{201}\text{Hg} \text{‰}$	$2\sigma \text{‰}$	N
SW China	Permian	sub-bituminous	0.42	−0.93	0.10	−0.04	0.04	0.03	0.04	2
		bituminous	0.36	−0.85	0.76	−0.03	0.09	−0.05	0.06	12
		anthracite	0.41	−0.59	1.16	−0.01	0.11	−0.03	0.16	2
eastern part of Northern China	Triassic	bituminous	0.32	−1.53	0.10	−0.08	0.06	0.02	0.10	1
	Carboniferous	bituminous	0.23	−0.74	1.05	−0.01	0.11	−0.02	0.10	5
		anthracite	0.29	−0.26	0.20	−0.05	0.04	−0.07	0.06	1
		bituminous	0.24	−0.79	0.33	−0.04	0.17	−0.05	0.15	9
		anthracite	0.41	−0.71	0.68	0.06	0.13	0.02	0.14	2
other parts of China	Carboniferous	sub-bituminous	0.11	−1.00	0.62	−0.10	0.18	−0.16	0.22	1
		bituminous	0.20	−0.95	1.16	−0.02	0.07	−0.03	0.11	6
		anthracite	0.19	−1.04	0.92	−0.04	0.07	0.00	0.11	2
	Jurassic	lignite	0.07	−1.13	0.30	0.15	0.08	0.11	0.06	1
		sub-bituminous	0.08	−0.76	0.30	−0.27	0.27	−0.23	0.24	2
		bituminous	0.08	−0.98	0.76	−0.26	0.23	−0.24	0.19	4
	Permian	sub-bituminous	0.30	−0.65	0.22	−0.10	0.02	−0.14	0.1	1
		bituminous	0.15	−1.61	0.71	−0.06	0.53	−0.05	0.54	6
		anthracite	0.15	−1.52	1.66	−0.16	0.55	−0.14	0.47	4

$$\Delta^{199}\text{Hg} \approx \delta^{199}\text{Hg} - (\delta^{202}\text{Hg} \times 0.2520) \quad (2)$$

$$\Delta^{200}\text{Hg} \approx \delta^{200}\text{Hg} - (\delta^{202}\text{Hg} \times 0.5024) \quad (3)$$

$$\Delta^{201}\text{Hg} \approx \delta^{201}\text{Hg} - (\delta^{202}\text{Hg} \times 0.7520) \quad (4)$$

The reproducibility was assessed by measuring replicate sample digests (typically  $n = 2$ ). We also analyzed the UM-Almadén as a secondary standard in the same way as other samples in each analytical session. The overall average and uncertainty of UM-Almadén ( $\delta^{202}\text{Hg}$ ,  $-0.57 \pm 0.10\text{‰}$ ;  $\Delta^{199}\text{Hg}$ ,  $-0.02 \pm 0.07\text{‰}$ ;  $\Delta^{201}\text{Hg}$ ,  $0.01 \pm 0.07\text{‰}$ ;  $2\sigma$ ,  $n = 12$ ) agreed well with Blum and Bergquist.<sup>43</sup> The isotopic composition of NIST SRM 2711 ( $\delta^{202}\text{Hg}$ ,  $-0.27 \pm 0.09\text{‰}$ ;  $\Delta^{199}\text{Hg}$ ,  $-0.19 \pm 0.05\text{‰}$ ;  $\Delta^{201}\text{Hg}$ ,  $-0.20 \pm 0.04\text{‰}$ ,  $2\sigma$ ,  $n = 6$ ) was comparable with previous

studies,<sup>20,44</sup> indicating that the matrix effect is limited in the present study. Uncertainties reported in this study correspond to the larger value of either (1) the external precision of repeated measurements of the UM-Almadén or (2) the uncertainty from measuring replicate digests.

## RESULTS AND DISCUSSION

**Total Hg Concentrations in Coal.** The THg concentrations of the 61 Chinese coals range from 0.05 to  $0.78 \mu\text{g g}^{-1}$ , with an arithmetic mean (AM) of  $0.26 \pm 0.16 \mu\text{g g}^{-1}$  ( $2\sigma$ ,  $n = 61$ ). The THg concentration in the measured coals exhibits a log-normal distribution pattern, which indicates a geometric mean (GM) of  $0.22 \mu\text{g g}^{-1}$ . Our data is comparable with previous studies on Chinese coals.<sup>45–47</sup> For instance, Zhang et

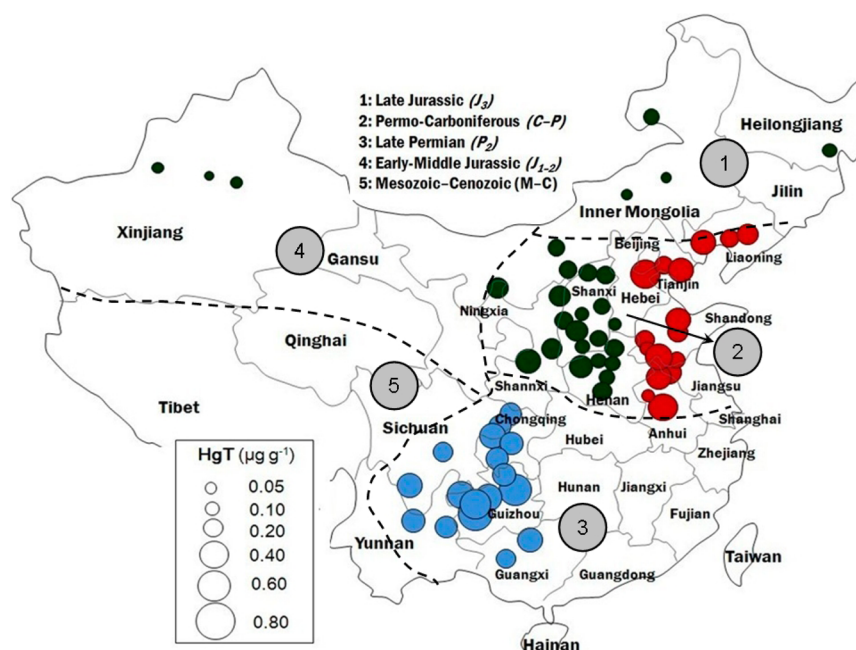


**Figure 1.** Spatial distribution of total Hg concentration in coals. Red circles represent coal samples collected from eastern part of northern China; Blue circles represent coal samples collected from SW China; Green circles represent coal samples collected from other parts of China.

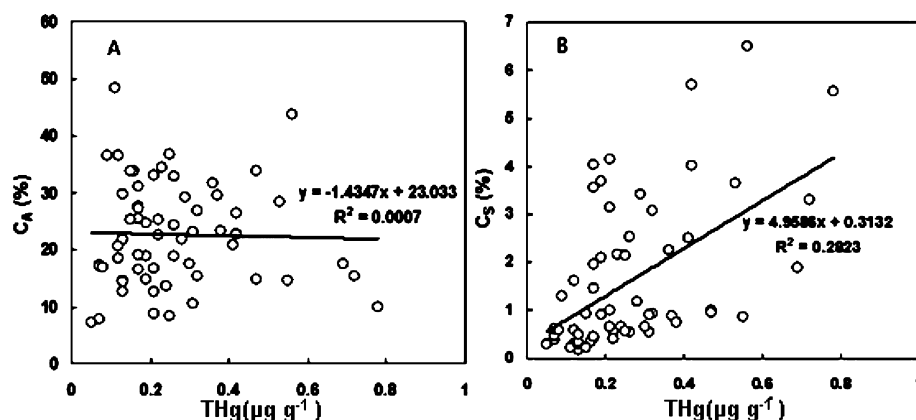


**Figure 2.** Correlation between total Hg concentration and (A) total ash content and (B) total sulfur content.

al.<sup>45</sup> estimated an average THg of  $0.16 \mu\text{g g}^{-1}$  ( $n = 1413$ ) in Chinese coals. Wang et al.<sup>46</sup> summarized the published THg data of 234 coals in China and estimated an AM THg of  $0.22 \mu\text{g g}^{-1}$ . Ren et al.<sup>47</sup> estimated an AM THg of  $0.20 \mu\text{g g}^{-1}$  for 1413 coals from China.

**Relations between Total Hg concentrations, Coal Ranks, and Coal Forming Periods.** Hg concentrations and occurrence in coal deposits is complex and controlled by many factors, e.g., coal ranks and geological backgrounds.<sup>48</sup> Generally, the higher rank a coal is, the deeper the coal was buried, and therefore the higher temperature the coal experienced during and after burial. Low rank coals (e.g., lignite and sub-bituminous) are formed during geothermal metamorphism and are characterized by high moisture levels and low carbon content.<sup>49</sup> Higher rank coals (e.g., bituminous and anthracite) are subjected to the telemagmatic metamorphism, which refers to the intrusion of deep-seated plutonic bodies under the coal-bearing strata.<sup>49</sup> The plutonic body transports hydrothermal fluids and brings Hg into the coal-bearing strata. Generally, the greater telemagmatic metamorphism of the coals suffered, the higher ranks the coals would have, and the more hydrothermal

Hg could be transported to coals.<sup>48</sup> As shown in Table 1, most coals show relatively high coal ranks, and the THg concentrations in coal seem to increase with the increase of coal ranks. Zheng et al.<sup>50</sup> also observed a similar pattern in 1283 Chinese coals: lignite ( $0.09 \mu\text{g g}^{-1}$ ,  $n = 903$ ) < bituminous ( $0.30 \mu\text{g g}^{-1}$ ,  $n = 138$ ) < anthracite ( $0.84 \mu\text{g g}^{-1}$ ,  $n = 217$ ). The connection between THg concentrations in coal and coal rank implies that the coal may absorb Hg during telemagmatic metamorphism processes. The THg concentrations in coals vary remarkably for different coal forming periods (Table 2), and Jurassic coals, which generally characterized by lower coal ranks, have the lowest THg.

**Spatial Distribution Patterns of Total Hg Content in Coals.** A decreased pattern of THg concentration in coal was observed in coals from Southern China to Northern China, as shown in Figure 1. Similar decreasing patterns of THg concentrations in coals from Southern China to Northern China have been observed by several studies.<sup>46,50</sup> For instance, the P coal producing region in SW China, which includes Guizhou, Chongqing, Sichuan, Yunnan, and Guangxi provinces, has the highest GM THg concentration in coal ( $0.37 \mu\text{g g}^{-1}$ ,  $n$



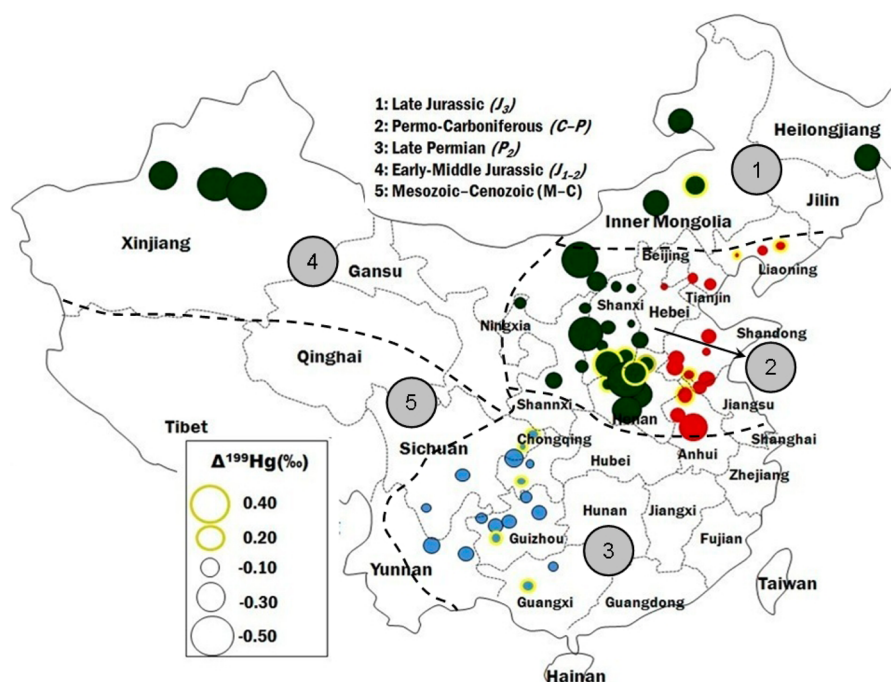


**Figure 3.** Spatial distribution of  $\Delta^{199}\text{Hg}$  in coals. Red circles represent coal samples collected from eastern part of Northern China; blue circles represent coal samples collected from SW China; green circles represent coal samples collected from other parts of China.

= 17); the C–P coal producing region in eastern part of northern China, which mainly includes Hebei, Beijing, Liaoning, Shandong, Jiangsu, Anhui, and Henan provinces, has an intermediate GM THg concentration in coal ( $0.25 \mu\text{g g}^{-1}$ ,  $n = 17$ ), and coal samples collected from other part of Northern China, which mainly includes Shanxi, Shaanxi, Henan, Inner Mongolia, Ningxia, Xinjiang, and Heilongjiang provinces, have the lowest GM THg concentration in coal ( $0.14 \mu\text{g g}^{-1}$ ,  $n = 27$ ). The spatial variations of THg concentrations in coals from China may be controlled by the magnitude and range of metamorphism and hydrothermal activities. Frequent magmatic activities, especially during Yanshan Orogeny at  $\sim 165 \pm 5$  Ma and 83 Ma, occurred throughout China. During Yanshan Orogeny, Eastern and Southern China were demonstrated to experience greater magmatic activities than the western and Northern China, which led to an increased pattern of coal ranks from Western China to Eastern China, and from Southern China to Northern China.<sup>49</sup> Hydrothermal fluids that increased the rank of coal played a role in enriching Hg in coal from Eastern and Southern China.

**Possible Modes of Occurrence of Hg in Coals.** There are at least three fractions of Hg in coals, i.e., clay-bound, organic-bound, and sulfide-bound.<sup>51</sup> In this study, the poor correlation ( $r^2 = 0.0007$ ,  $p < 0.05$ ,  $t$ -test) between  $C_A$  and THg in coals implies that the clays-bound Hg may not be the primary form of Hg in coals (Figure 2A). Hg has a strong affinity to organic matter and sulfur in coals.<sup>52</sup> The positive correlation between THg and  $C_S$  (Figure 2B:  $r^2 = 0.245$ ,  $p < 0.05$ ,  $t$ -test) in coal samples suggests that sulfide-bound Hg is an important mode of occurrence of Hg in coals. In high-sulfur coals, the most likely mode of occurrence of Hg in coal is sulfide minerals (e.g., pyrite), which are known as the dominant hosts of a suite of trace elements including Hg, Mo, Se, Cu, Tl, etc.<sup>53</sup> However, in low-sulfur coals, of which THg concentrations were generally low, organic-bound Hg may be the most

important fraction in coal. Evidently, the lower the sulfur contents of the coal, the greater the potential contribution of organic-bound Hg to the total Hg.<sup>48</sup>

Generally, the areas with high THg concentrations coincide geographically with high sulfur coal areas. For instance, for the SW China coal producing regions, such as the Guizhou, Chongqing, Sichuan, Yunnan, and Guangxi provinces, coal samples are generally characterized as the highest THg ( $0.37 \mu\text{g g}^{-1}$ ,  $n = 17$ ). The elevated THg concentration in coals from this region is demonstrated to be controlled by the low-temperature thermal fluid activities.<sup>53–55</sup> In this study, coals from SW China were characterized by high  $C_S$  (mean  $C_S = 2.90 \pm 1.89\%$ ,  $2\sigma$ ,  $n = 17$ ) compared with coals from other regions (mean  $C_S = 1.10 \pm 1.02\%$ ,  $2\sigma$ ,  $n = 44$ ). In contrast to the SW China coals, coals from Northern China (especially Xinjiang, Inner Mongolia, Shanxi, Shaanxi, Ningxia, and Henan provinces) have the lowest THg ( $0.16 \pm 0.08 \mu\text{g g}^{-1}$ ,  $2\sigma$ ,  $n = 27$ ). Coal samples in these regions are characterized by low  $C_S$  content (Table S1, Supporting Information), indicating the coal strata here experienced less impact from hydrothermal activities.<sup>56</sup>

**Mass Independent Fractionation of Hg Isotopes.** The isotopic compositions of Hg in the coal samples is shown in Table S1 (Supporting Information). The large variations of  $\Delta^{199}\text{Hg}$  values (Figure 3;  $-0.44$  to  $+0.38\%$ ) were demonstrated to be an important feature for the investigated coals. At least two understood mechanisms that can cause Hg MIF are the nuclear volume effect (NVE)<sup>57,58</sup> and the magnetic isotope effect (MIE).<sup>5,59</sup> The NVE originates from the effect of nuclear volume on electrons. Variations in nuclear size and shape change the nuclear charge distribution, which results in a slightly different electrostatic field to interact with electrons having a high density at the nucleus (i.e., s orbital electrons). Schauble<sup>57</sup> calculated contributions of NVE to isotope fractionation factors for various species of Hg and Tl and predicted generally higher contributions of NVE to isotope fractionation relative to MDF effects. The NVE has been

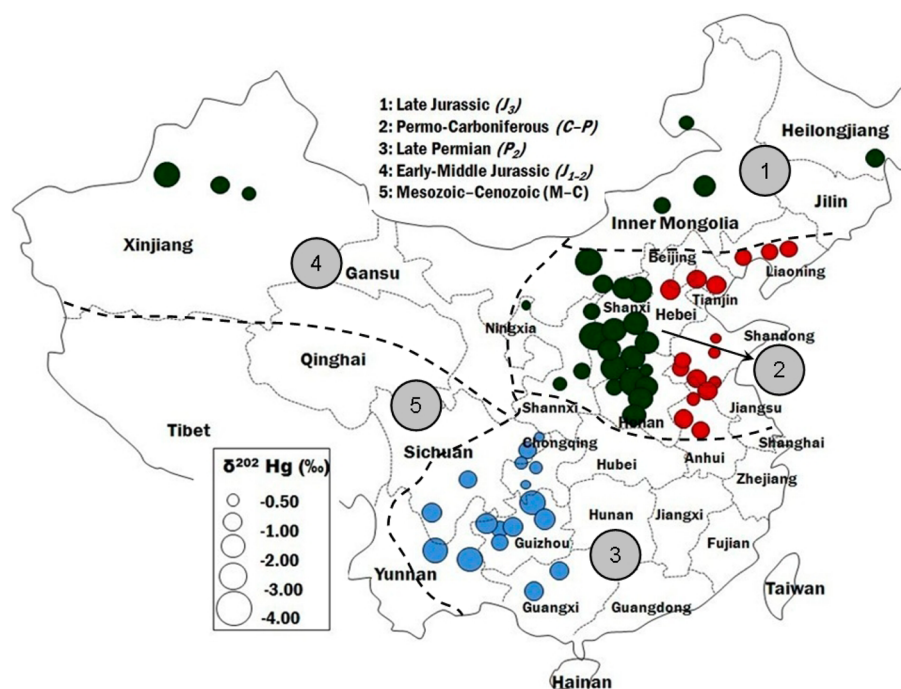


**Figure 4.** Spatial distribution of  $\delta^{202}\text{Hg}$  in coals. Red circles represent coal samples collected from eastern part of Northern China; blue circles represent coal samples collected from SW China; green circles represent coal samples collected from other parts of China.

observed by several laboratory experiments, e.g., nonphoto reduction of dissolved Hg species,<sup>58</sup> evaporation,<sup>29</sup> and Hg–thiol complexation.<sup>30</sup> The MIE is a kinetic fractionation that appears to occur primarily during photochemical radical pair reactions.<sup>5,27,60</sup> It should be mentioned that the NVE and MIE could be differentiated according to their  $\Delta^{199}\text{Hg}/\Delta^{201}\text{Hg}$  ratios. Plotting  $\Delta^{199}\text{Hg}$  versus  $\Delta^{201}\text{Hg}$  reveals a significant difference for MIE ( $\Delta^{199}\text{Hg}/\Delta^{201}\text{Hg}$ : 1.0–1.3) versus that of NVE ( $\Delta^{199}\text{Hg}/\Delta^{201}\text{Hg}$ : >1.6). For instance,  $\text{Hg}^0$  volatilization experiments demonstrated  $\Delta^{199}\text{Hg}/\Delta^{201}\text{Hg}$  of 2.0 for NVE.<sup>29</sup> Nonphoto reduction of  $\text{Hg}^{2+}$  induces NVE with  $\Delta^{199}\text{Hg}/\Delta^{201}\text{Hg}$  of 1.5 to 1.61.<sup>5,27,58</sup> Equilibrium Hg–thiol complexation caused NVE with  $\Delta^{199}\text{Hg}/\Delta^{201}\text{Hg}$  of 1.54.<sup>30</sup> The MIE has been shown to occur during the photochemical reactions of aqueous Hg in the presence of dissolved organic carbon.<sup>5,27,60</sup> Laboratory experiments have demonstrated that photoreduction of aqueous  $\text{Hg}^{2+}$  and photodegradation of  $\text{MeHg}$  in the presence of natural DOC can produce  $\Delta^{199}\text{Hg}/\Delta^{201}\text{Hg}$  ratios of 1.0 and 1.36, respectively.<sup>5</sup> As shown in Figure S3 (Supporting Information), a linear regression of  $\Delta^{199}\text{Hg}$  and  $\Delta^{201}\text{Hg}$  for all coals yields a slope of  $1.03 \pm 0.07$  ( $2\sigma$ ), which is consistent with that of the MIE and previous observation of coal samples, indicating a portion of Hg in coals may be subject to photochemical processes in the surface environment prior to coalification.<sup>18,19</sup> Large variations of MIF with  $\Delta^{199}\text{Hg}/\Delta^{201}\text{Hg}$  of  $\sim 1$  have been observed in the modern environment on the global scale (e.g., soils/sediments, plants, coal, atmospheric Hg species and precipitations), which also suggest that aqueous Hg photoreduction could be the main process inducing Hg MIF.<sup>5,14–16,18–20,31,33,34,61–64</sup>

**Spatial Distribution of Hg Isotopes and Potential Hg Sources.** In addition to MIF, Hg in coal samples also show large variations in  $\delta^{202}\text{Hg}$  values (Figure 4;  $-2.36$  to  $-0.14\text{‰}$ ). One possible explanation for the variation of  $\delta^{202}\text{Hg}$  in coals is isotopic fractionation during coalification processes. Coal begins as peat. Remobilization of Hg during the peat stage

can be caused by multiple processes, including microbial (e.g., microreduction,<sup>23,24</sup> methylation/demethylation<sup>25,26</sup>) and abiotic (e.g., photoreduction,<sup>5,27,60</sup> volatilization,<sup>28</sup> evaporation,<sup>29</sup> adsorption,<sup>30</sup> and leaching<sup>71</sup>) processes, during which isotope fractionation of Hg has been documented. However, coal-forming peats buried under mineral sediments (e.g., clay, silt, and sand) are subject to anoxic conditions, in which most Hg compounds (e.g.,  $\text{HgS}$ ) are highly stable and insoluble.<sup>48</sup> In addition, the amount of Hg remobilized in coals is considered to be minimal due to the strong adsorption of Hg by organic matter. Hence, we speculate coalification processes may potentially not be capable of altering the Hg isotopic compositions of coals.

Alternatively, the variations of Hg isotopes in coals can be explained by mixing of different sources with distinct Hg isotopic signatures. Coal received Hg from biogenic sources and geogenic Hg sources,<sup>72</sup> and these Hg sources can be distinguished by different Hg signatures.<sup>19</sup> Biologically sourced Hg has significant MIF signatures,<sup>5,22,61–63,69</sup> whereas geological sources (e.g., volcanoes, crustal sources and hydrothermal fluids) is characterized by lower MIF signatures ( $\Delta^{199}\text{Hg}$ :  $< \pm 0.2\text{‰}$ ).<sup>7–14,17</sup> Hg MIF may serve as a tool in understanding the origins of coal. Dissolved organic matter (DOM) plays a critical role in controlling the photoreduction processes that cause Hg MIF.<sup>5</sup> DOM contains a large abundance of oxygen functional groups (e.g., carboxyl or phenol groups) and less reduced sulfur compounds (e.g., thiol and disulfide/disulfane functional groups).<sup>27,60</sup> The MIF of Hg isotopes is largely controlled by the ligands to which Hg is bound.<sup>5,27,60</sup> Photoreduction of  $\text{Hg}^{2+}$  driven by natural DOM showed negative MIF in the product  $\text{Hg}^0$  and positive MIF in the reactant,<sup>5,27</sup> whereas photoreduction of  $\text{Hg}^{2+}$  driven by thiols led to positive MIF in the product  $\text{Hg}^0$  and negative MIF in the reactant.<sup>58</sup> Photoreduction derived by natural DOM is the main process to produce significant MIF in natural reservoirs.<sup>62</sup> Positive MIF signatures have been observed in

fresh water,<sup>65</sup> aquatic organisms,<sup>5,22</sup> ocean sediments,<sup>66</sup> and ocean black shale;<sup>67</sup> however, negative MIF signatures have been detected in terrestrial soil<sup>18,68</sup> and plants.<sup>61,63,69</sup> Coal deposits are genetically divided into two broad groups: the humic coals and the sapropelic coals.<sup>70</sup> Humic coals originated in swamps similar to the present-day peat bogs, reflecting the lush vegetation in ancient coal-forming environments. Humic coals receive Hg from decayed plants and are probably characterized by negative MIF. Sapropelic coal refers to organic matter accumulation in shallow- to deep-marine basins and lagoons,<sup>70</sup> which receive Hg mainly from aquatic water and organisms<sup>19</sup> and may be characterized by positive MIF.

In this study, Hg isotopic compositions showed insignificant correlations to both THg and  $C_A$  values (Figure S4, Supporting Information). Hg isotopic compositions in coals also showed no clear trends with the coal ranks (Table 1) and the coal forming ages (Table 2). Interestingly, Hg isotopic signatures in coal seem to vary among different coal producing regions (Figures 3 and 4). On the basis of the combination of THg concentration in coal, Hg isotopic signatures, and the geological characteristics, we try to discriminate the potential sources of Hg in coals from different coal producing regions. For the *P* coal producing region in SW China (e.g. Guizhou, Chongqing, Sichuan, Yunnan, and Guangxi provinces), coal samples are generally characterized by the higher  $\delta^{202}\text{Hg}$  ( $-0.87 \pm 0.40\%$ ,  $2\sigma$ ,  $n = 17$ ) and negligible MIF signatures ( $\Delta^{199}\text{Hg} = -0.03 \pm 0.04\%$ ,  $2\sigma$ ,  $n = 17$ ). The elevated THg in SW China coals could be related to the low-temperature thermal fluid activities.<sup>53–55</sup> Previous studies demonstrated Hg in coal has a strong affinity with sulfur in Guizhou coals and the dominant mode of occurrence of Hg is sulfide minerals.<sup>53–55</sup> In this study, coals from SW China were characterized by high  $C_S$  content (mean  $C_S = 2.90 \pm 1.89\%$ ,  $2\sigma$ ,  $n = 17$ ) compared with coals from other regions (mean  $C_S = 1.10 \pm 1.02\%$ ,  $2\sigma$ ,  $n = 44$ ). Meanwhile, the higher  $\delta^{202}\text{Hg}$  ( $-0.87 \pm 0.40\%$ ,  $2\sigma$ ,  $n = 17$ ) and negligible MIF in SW China coals is comparable with published data on geogenic Hg ( $\delta^{202}\text{Hg}$ :  $\sim -0.70\%$ ;  $\Delta^{199}\text{Hg}$ :  $\sim 0$ ),<sup>7–14,17</sup> indicating the important contribution of geogenic source to Hg in coals of this region.

For the C–P coal producing region in eastern part of Northern China (e.g., Hebei, Beijing, Liaoning, Shandong, Jiangsu, Anhui, and Henan provinces), coal samples are characterized by an intermediate GM THg concentration ( $0.37 \mu\text{g g}^{-1}$ ,  $n = 17$ ) and the highest  $\delta^{202}\text{Hg}$  ( $-0.73 \pm 0.33\%$ ,  $2\sigma$ ,  $n = 17$ ), and with negligible MIF ( $\Delta^{199}\text{Hg} = -0.02 \pm 0.08\%$ ,  $2\sigma$ ,  $n = 17$ ). In eastern part of Northern China, frequent continental volcanic and intrusive activities during Mesozoic and Cenozoic Eras led to a wide distribution of contact metamorphism of coal.<sup>73</sup> Igneous intrusions affect organic matter, which led to elevated coal ranks, and brought Hg into the coal-bearing strata.<sup>48</sup> For example, high values of Hg observed in coals of the Huaibei Coalfield (Anhui province) are attributed to Hg enrichment by magmatic intrusions.<sup>74</sup> Similar to coal samples from SW China, the insignificant MIF in coals of this region also indicates the dominance of geogenic Hg in coals.

Coals from other part of Northern China (e.g., Xinjiang, Inner Mongolia, Shanxi, Shannxi, Ningxia, and Henan provinces) exhibit much lower  $\delta^{202}\text{Hg}$  values ( $-1.19 \pm 0.56\%$ ,  $2\sigma$ ,  $n = 27$ ) and significant MIF ( $\Delta^{199}\text{Hg} = -0.10 \pm 0.19\%$ ,  $2\sigma$ ,  $n = 27$ ) in coals. As shown in Table 2, coal samples in these regions are characterized by the lower THg and the lowest  $C_S$  content, which probably indicates less hydrothermal

activity imprint.<sup>56</sup> Similar to the modern plants<sup>61–63,69</sup> and peat samples,<sup>75,76</sup> the coals in these regions have significant MIF of Hg isotopes with a  $\Delta^{199}\text{Hg}/\Delta^{201}\text{Hg}$  ratio of  $\sim 1.0$  (Figure S3, Supporting Information). Hence, we hypothesized that the biogenic Hg may be the dominant source of Hg in coals of these regions and Hg is mainly associated with organic matters.

**Estimation of Hg Isotopic Signature of Coal Combustion in China.** Coal combustion from China is estimated to be an important source of Hg emissions in the world.<sup>3,4</sup> Using Hg isotope as a tool to discriminate Hg emissions from coal combustion in China requires (i) well-established Hg isotopic compositions of coals in China and (ii) well-founded Hg isotope fractionation constraints during coal combustion processes. On the basis of our hitherto data in coal samples (Table S2, Supporting Information), the average Hg isotopic compositions ( $\delta^{202}\text{Hg}$  and  $\Delta^{199}\text{Hg}$ ) in coals from China were calculated using the following equations:

$$\delta^{202}\text{Hg}_T = \frac{\sum_{i=18} M_i \cdot C_i \cdot \delta^{202}\text{Hg}_i}{\sum_{i=18} M_i \cdot C_i} \quad (5)$$

$$\Delta^{199}\text{Hg}_T = \frac{\sum_{i=18} M_i \cdot C_i \cdot \Delta^{199}\text{Hg}_i}{\sum_{i=18} M_i \cdot C_i} \quad (6)$$

where  $i$  indicates the province ( $i = 18$ ) in which the coal samples were collected in the present study;  $M_i$  represents the amount of coal produced in province  $i$ ;  $C_i$  represents the GM THg values of coals in province  $i$ ;  $\delta^{202}\text{Hg}_i$  represents the mean  $\delta^{202}\text{Hg}$  value of coals in province  $i$ ;  $\Delta^{199}\text{Hg}_i$  represents the mean  $\Delta^{199}\text{Hg}$  value of coals in province  $i$ . The  $\delta^{202}\text{Hg}_T$  and  $\Delta^{199}\text{Hg}_T$  represent the weighted average  $\delta^{202}\text{Hg}$  and  $\Delta^{199}\text{Hg}$  values of coals in China, respectively. In this study, the amount of coal produced in each province in China in 2011 is used.<sup>77</sup> In 2011, the total amount of coal produced in the 18 provinces is  $3592.2 \times 10^6$  tons, which represents 93.8% of the total coal production in China ( $3830.3 \times 10^6$  tons).<sup>77</sup> On the basis of the eqs 5 and 6, the Hg isotopic compositions of coals in 18 provinces in China was estimated to be  $\delta^{202}\text{Hg}_T = -1.00\%$  and  $\Delta^{199}\text{Hg}_T = -0.05\%$ , respectively. Hence, we postulated the  $\delta^{202}\text{Hg}_T = -1.00\%$  and  $\Delta^{199}\text{Hg}_T = -0.05\%$  as the average Hg isotopic compositions of coals in China.

During coal combustion, Hg in coals is liberated as gaseous  $\text{Hg}^0$ , reactive gaseous Hg, and particulate Hg. All of these forms of Hg will travel different distances in the atmosphere, impacting Hg deposition on different scales. Sun et al.<sup>21</sup> investigated Hg isotope fractionation between feed coal and coal combustion products (e.g., bottom ash, fly ash, and flue gas desulphurization byproduct gypsum) in six utility boilers of two large power plants in Huainan City, China. According to Sun et al.,<sup>21</sup> no MIF was observed during the transport and transformation of Hg inside the boilers. However, based on an isotope mass balance model, the gaseous  $\text{Hg}^0$  emitted is expected to be enriched in heavy Hg isotopes (up to  $+0.3\%$  in  $\delta^{202}\text{Hg}$ ) compared to the feed coals.<sup>21</sup> Hence, we concluded that  $\text{Hg}^0$  emissions from coal combustion in China could be diagnostic by its Hg isotopic signatures ( $\delta^{202}\text{Hg}$ ,  $\sim -0.70\%$  and  $\Delta^{199}\text{Hg}$ ,  $\sim -0.05\%$ ). It should be noted almost all of the coal mined in China burned domestically. Significant exports of coal to other countries could impact the estimated isotopic composition of burned coal. This study does not attempt to investigate changes in isotopic composition that likely occur during coal processing, combustion, and atmospheric transport.



Meanwhile, it is likely that Hg fractionation occurs within power plants depending on a number of factors including type and efficiency of air pollution control devices, chemical composition of coal (e.g., halogen, ash concentration), temperature in the flue gas, etc. Therefore, much more research is needed before we can accurately estimate the isotopic composition of emissions from China based on measurements of isotopic composition of coals.

## ■ ASSOCIATED CONTENT

### ● Supporting Information

Figures of main coal producing regions in China and the sampling sites, correlation between added-Hg and measured-Hg using standard-addition method, correlation between  $\Delta^{201}\text{Hg}$  versus  $\Delta^{199}\text{Hg}$  in Chinese coals, correlations between Hg isotopic compositions and THg and CA values; tables of sample information, total Hg concentration and Hg isotopic composition and the amount of coal production, mean THg and isotopic composition of Hg in coals from different provinces in China. This material is available free of charge via the Internet at <http://pubs.acs.org>.

## ■ AUTHOR INFORMATION

### Corresponding Author

\*Xinbin Feng. Phone: +86-851-5891356. Fax: +86-851-5891609. E-mail: [fengxinbin@vip.skleg.cn](mailto:fengxinbin@vip.skleg.cn).

### Notes

The authors declare no competing financial interest.

## ■ ACKNOWLEDGMENTS

This research was funded by National “973” Program (2013CB430001), Natural Science Foundation of China (41303014, 41021062, and 41120134005) and Hundred Talent Plan of Chinese Academy of Sciences. We thank Professors Zheng B.S. and Zhu J.M. for providing the coal samples. We also acknowledge Dr. Yu B. and Dr. Du B.Y. from State Key Laboratory of Environmental Geochemistry (Chinese Academy of Sciences) for isotope analysis assistance. Finally, Prof. Zhu C. from Department of Geological Science (Indiana University) and two anonymous reviewers are thanked for their relevant comments that have largely improved the quality of our paper.

## ■ REFERENCES

- (1) Fitzgerald, W. F.; Engstrom, D. R.; Mason, R. P.; Nater, E. A. The case for atmospheric mercury contamination in remote areas. *Environ. Sci. Technol.* **1998**, *32*, 1.
- (2) Pirrone, N.; Cinnirella, S.; Feng, X.; Finkelman, R. B.; Friedli, H. R.; Leaner, J.; Mason, R.; Mukherjee, A. B.; Stracher, G. B.; Streets, D. G.; Telmer, K. Global mercury emissions to the atmosphere from anthropogenic and natural sources. *Atmos. Chem. Phys.* **2010**, *10*, 5951–5964.
- (3) Streets, D. G.; Hao, J. M.; Wu, Y.; Jiang, J. K.; Chan, M.; Tian, H. Z.; Feng, X. B. Anthropogenic mercury emissions in China. *Atmos. Environ.* **2005**, *39*, 7789–7806.
- (4) Wu, Y.; Wang, S.; Streets, D. G.; Hao, J.; Chan, M.; Jiang, J. Trends in anthropogenic mercury emissions in China from 1995 to 2003. *Environ. Sci. Technol.* **2006**, *40* (17), 5312–5318.
- (5) Bergquist, B. A.; Blum, J. D. Mass-dependent and -independent fractionation of Hg isotopes by photo reduction in aquatic systems. *Science* **2007**, *318*, 19.
- (6) Sonke, J. E.; Blum, J. D. Advances in mercury stable isotope biogeochemistry. *Chem. Geol.* **2013**, *336*, 1–4.
- (7) Hintelmann, H.; Lu, S. Y. High precision isotope ratio measurements of mercury isotopes in cinnabar ores using multi-collector inductively coupled plasma mass spectrometry. *Analyst* **2003**, *128*, 635–639.
- (8) Smith, C. N.; Keslera, S. E.; Blum, J. D.; Rytuba, J. J. Isotope geochemistry of mercury in source rocks, mineral deposits and spring deposits of the California Coast Ranges, USA. *Earth Planet. Sci. Lett.* **2008**, *269*, 399–407.
- (9) Stetson, S. J.; Gray, J. E.; Wanty, R. B.; Macalady, D. L. Isotopic variability of mercury in ore, mine-waste calcine, and leachates of mine-waste calcine from areas mined for mercury. *Environ. Sci. Technol.* **2009**, *43* (19), 7331–7336.
- (10) Sonke, J. E.; Schaefer, J.; Chmieleff, J.; Audry, S.; Blanc, G.; Dupre, B. Sedimentary mercury stable isotope records of atmospheric and riverine pollution from two major European heavy metal refineries. *Chem. Geol.* **2010**, *279*, 90–100.
- (11) Smith, C. N.; Kesler, S. E.; Klaue, B.; Blum, J. D. Mercury isotope fractionation in fossil hydrothermal systems. *Geology* **2005**, *33*, 825–828.
- (12) Sherman, L. S.; Blum, J. D.; Nordstrom, D. K.; McCleskey, R. B.; Barkay, T.; Vetriani, C. Mercury isotopic composition of hydrothermal systems in the Yellowstone Plateau volcanic field and Guaymas Basin sea-floor rift. *Earth Planet. Sci. Lett.* **2009**, *29*, 86–96.
- (13) Foucher, D.; Ogring, N.; Hintelmann, H. Tracing mercury contamination from the Idrija Mining Region (Slovenia) to the Gulf of Trieste using Hg isotope ratio measurements. *Environ. Sci. Technol.* **2009**, *43*, 33–39.
- (14) Feng, X. B.; Foucher, D.; Hintelmann, H.; Yan, H. Y.; He, T. R.; Qiu, G. L. Tracing mercury contamination sources in sediments using mercury isotope compositions. *Environ. Sci. Technol.* **2010**, *44*, 3363–3368.
- (15) Sonke, J. E.; Schaefer, J.; Chmieleff, J.; Audry, S.; Blanc, G.; Dupre, B. Sedimentary mercury stable isotope records of atmospheric and riverine pollution from two major European heavy metal refineries. *Chem. Geol.* **2010**, *279*, 90–100.
- (16) Liu, J.; Feng, X.; Yin, R.; Zhu, W.; Li, Z. Mercury distributions and mercury isotope signatures in sediments of Dongjiang River, the Pearl River Delta, China. *Chem. Geol.* **2011**, *287* (1–2), 81–89.
- (17) Yin, R. S.; Feng, X. B.; Wang, J. B.; Bao, Z. D.; Yu, B.; Chen, J. B. Mercury isotope variations between bioavailable mercury fractions and total mercury in mercury contaminated soil in Wanshan Mercury Mine, SW China. *Chem. Geol.* **2013**, *336*, 80–86.
- (18) Biswas, A.; Blum, J. D.; Bergquist, B. A.; Keeler, G. J.; Xie, Z. Q. Natural mercury isotope variation in coal deposits and organic soils. *Environ. Sci. Technol.* **2008**, *42*, 8303–8309.
- (19) Leticariu, L.; Blum, J.; Gleason, J. Mercury isotopic evidence for multiple mercury sources in coal from the Illinois Basin. *Environ. Sci. Technol.* **2011**, *45* (4), 1724–1729.
- (20) Sherman, L. S.; Blum, J. D.; Keeler, G. J.; Demers, J. D.; Dvonch, J. T. Investigation of local mercury deposition from a coal-fired power plant using mercury isotopes. *Environ. Sci. Technol.* **2012**, *46* (1), 382–390.
- (21) Sun, R.; Heimbürger, L.-E.; Sonke, J. E.; Liu, G.; Amouroux, D.; Berail, S. Mercury stable isotope fractionation in six utility boilers of two large coal-fired power plants. *Chem. Geol.* **2013**, *336*, 103–111.
- (22) Jackson, T. A.; Whittle, D. M.; Evans, M. S.; Muir, D. C. G. Evidence for mass-independent and mass-dependent fractionation of the stable isotopes of mercury by natural processes in aquatic ecosystems. *Appl. Geochem.* **2008**, *23*, 547–571.
- (23) Kritee, K.; Blum, J. D.; Johnson, M. W.; Bergquist, B. A.; Barkay, T. Mercury stable isotope fractionation during reduction of Hg(II) to Hg(0) by mercury resistant microorganisms. *Environ. Sci. Technol.* **2007**, *41*, 1889–1895.
- (24) Kritee, K.; Blum, J. D.; Barkay, T. Mercury stable isotope fractionation during reduction of Hg(II) by different microbial pathways. *Environ. Sci. Technol.* **2008**, *42*, 9171–9177.
- (25) Rodríguez-González, P.; Epov, V. N.; Pecheyran, C.; Amouroux, D.; Donard, O. F. X. Species-Specific stable isotope fractionation of mercury during Hg(II) methylation by an anaerobic bacteria (*Desulfobulbus propionicus*) under dark conditions. *Environ. Sci. Technol.* **2009**, *43*, 9183–9188.



- (26) Kritee, K.; Barkay, T.; Blum, J. D. Mass dependent stable isotope fractionation of mercury during mer mediated microbial degradation of monomethylmercury. *Geochim. Cosmochim. Acta* **2009**, *73*, 1285–1296.
- (27) Zheng, W.; Hintelmann, H. Mercury isotope fractionation during photoreduction in natural water is controlled by its Hg/DOC ratio. *Geochim. Cosmochim. Acta* **2009**, *73*, 6704–6715.
- (28) Zheng, W.; Foucher, D.; Hintelmann, H. Mercury isotope fractionation during volatilization of Hg(0) from solution into the gas phase. *J. Anal. At. Spectrom.* **2007**, *22*, 1097–1104.
- (29) Estrade, N.; Carignan, J.; Sonke, J. E.; Donard, O. F. X. Mercury isotope fractionation during liquid–vapor evaporation experiments. *Geochim. Cosmochim. Acta* **2009**, *73*, 2693–2711.
- (30) Wiederhold, J. G.; Daniel, K.; Infante, I.; Bourdon, B.; Kretzschmar, R. Equilibrium mercury isotope fractionation between dissolved Hg(II) species and thiol-bound Hg. *Environ. Sci. Technol.* **2010**, *44*, 4191–4197.
- (31) Bergquist, B. A.; Blum, J. D. The odds and evens of mercury isotopes: applications of mass-dependent and mass-independent isotope fractionation. *Elements* **2009**, *5*, 353–357.
- (32) Yin, R. S.; Feng, X. B.; Shi, W. F. Application of the stable-isotope system to the study of sources and fate of Hg in the environment: A review. *Appl. Geochem.* **2010**, *25*, 1467–1477.
- (33) Gratz, L.; Keeler, G.; Blum, J.; Sherman, L. S. Isotopic composition and fractionation of mercury in Great Lakes precipitation and ambient air. *Environ. Sci. Technol.* **2010**, *44*, 7764–7770.
- (34) Chen, J. B.; Hintelmann, H.; Feng, X. B.; Dimock, B. Unusual fractionation of both odd and even mercury isotopes in precipitation from Peterborough, ON, Canada. *Geochim. Cosmochim. Acta* **2012**, *90*, 33–46.
- (35) State Bureau of Technical Supervision. GB 474–1996, *Preparation of coal sample*; Standardization Administration of the People's Republic of China: Beijing, 1996.
- (36) Wang, X.; Zhu, L.; Wang, J.. *The forming and distribution of coalfields in China*; Science Publishing House: Beijing, 1992 (in Chinese).
- (37) Luis, R.; Jesusa, R.; Isaac, A.; Laura, R.-C. Capability of selected crop plants for shoot mercury accumulation from polluted soils: phytoremediation perspectives. *Int. J. Phytorem.* **2007**, *9*, 1–13.
- (38) US EPA. *Method 1631: Revision B: Mercury in Water by Oxidation, Purge and Trap, and Cold Vapor Atomic Fluorescence Spectrometry*; EPA-821-R-99-005; United States Environmental Protection Agency, Office of Water: Washington, D.C., 1999; pp 1–33.
- (39) ASTM. ASTM D3177: *Standard Test Methods for total Sulfur in the Analysis Sample of Coal and Coke*; ASTM International: West Conshohocken, PA, 1989.
- (40) ASTM. ASTM D3174-93: *Standard Test Method for Ash in the Analysis Sample of Coal and Coke from Coal*; ASTM International: West Conshohocken, PA, 1993.
- (41) ASTM. ASTM D388-99e1: *Standard Classification of Coals by Rank*; ASTM International: West Conshohocken, PA, 1999.
- (42) Yin, R. S.; Feng, X. B.; Foucher, D.; Shi, W. F.; Zhao, Z. Q.; Wang, J. High precision determination of mercury isotope ratios using online mercury vapor generation system coupled with Multicollector Inductively Coupled Plasma-Mass Spectrometer. *Chin. J. Anal. Chem.* **2010**, *38* (7), 929–934.
- (43) Blum, J. D.; Bergquist, B. A. Reporting of variations in the natural isotopic composition of mercury. *Anal. Bioanal. Chem.* **2007**, *388*, 353–359.
- (44) Estrade, N.; Carignan, J.; Donard, O. F. Isotope tracing of atmospheric mercury sources in an urban area of northeastern France. *Environ. Sci. Technol.* **2010**, *44* (16), 6062–7.
- (45) Zhang, J. Y.; Ren, D. Y.; Xu, D. W. In: *Distribution of arsenic and mercury in Triassic coals from Longtoushan Syncline, Southeastern Guizhou, P. R. China: Prospects for Coal Science in 215 Century*; Li, B. Q., Liu, Z. Y., Eds.; Shanxi Science Technology Press: Shanxi, China, 1999; pp 153–156.
- (46) Wang, Q.; Shen, W.; Ma, Z. Estimation of mercury emission from coal combustion in China. *Environ. Sci. Technol.* **2000**, *34*, 2711–2713.
- (47) Ren, D. Y.; Zhao, F. H.; Dai, S.; Zhang, J. Y.; Luo, K. L. *Geochemistry of trace elements in coals*; The Science Press: Beijing, 2006; pp 268–279 (in Chinese).
- (48) Finkelman, R. B.; Bostick, N. H.; Dulong, F. T.; Senftle, F. E.; Thorpe, A. N. Influence of an igneous intrusion on the inorganic geochemistry of a bituminous coal from Pitkin County, Colorado. *Int. J. Coal Geol.* **1998**, *36*, 223–241.
- (49) Yang, Q. Superimposed metamorphism of Chinese coal. *Earth Sci. Frontiers.* **1999**, *6*, 1–8 (In Chinese with English Abstract).
- (50) Zheng, L.; Liu, G.; Chou, C.-L. The distribution, occurrence and environmental effect of mercury in Chinese coals. *Sci. Total Environ.* **2007**, *384*, 374–383.
- (51) Yudovich, Ya. E.; Ketris, M. P. Mercury in coal: a review Part 1 geochemistry. *Int. J. Coal Geol.* **2005**, *62*, 107–34.
- (52) Goodarzi, F. *Geology of trace elements in coal*. In: *Environmental Aspects of Trace Elements in Coal*; Swaine, D. J., Goodarzi, F., Eds.; Kluwer Academic Publishers: Dordrecht, The Netherlands, 1995; pp 51–75.
- (53) Feng, X. B.; Hong, Y. T. Modes of occurrence of mercury in coals from Guizhou People's Republic of China. *Fuel* **1999**, *78*, 1181–8.
- (54) Ding, Z. H.; Zheng, B. S.; Long, J. P.; Belkin, H. E.; Finkelman, R. B.; Chen, C. G. Geological and geochemical characteristics of high arsenic coals from endemic arsenosis areas in southwestern Guizhou Province China. *Appl. Geochem.* **2001**, *16*, 1353–60.
- (55) Dai, S.; Sun, Y.; Zeng, R. Enrichment of arsenic, antimony, mercury, and thallium in a Late Permian anthracite from Xingren, Guizhou, Southwest China. *Int. J. Coal Geol.* **2006**, *66*, 217–226.
- (56) Wang, M. S.; Zheng, B. S.; Wang, B. B.; Li, S. H.; Wu, D. S.; Hu, J. Arsenic concentrations in Chinese coals. *Sci. Total Environ.* **2006**, *357*, 96–102.
- (57) Schauble, E. A. Role of nuclear volume in driving equilibrium stable isotope fractionation of mercury, thallium, and other very heavy elements. *Geochim. Cosmochim. Acta* **2007**, *71*, 2170–2189.
- (58) Zheng, W.; Foucher, D.; Hintelmann, H. Nuclear field shift effect in isotope fractionation of mercury during abiotic reduction in the absence of light. *J. Phys. Chem. A* **2010b**, *114*, 4238–4245.
- (59) Buchachenko, A. L.; Ivanov, V. L.; Roznyatovskii, V. A.; Artamkina, G. A.; Vorobev, A. K.; Ustynuk, Y. A. Magnetic isotope effect for mercury nuclei in photolysis of bis(p-trifluoromethylbenzyl) mercury. *Dokl. Phys. Chem.* **2007**, *413*, 39–41.
- (60) Zheng, W.; Foucher, D.; Hintelmann, H. Isotope fractionation of mercury during its photochemical reduction by low-molecular-weight organic compounds. *J. Phys. Chem. A* **2010a**, *114*, 4246–4253.
- (61) Carignan, J.; Estrade, N.; Sonke, J. E.; Donard, O. F. X. Odd Isotope Deficits in Atmospheric Hg Measured in Lichens. *Environ. Sci. Technol.* **2009**, *243*, 5660–5664.
- (62) Sonke, J. E. A global model of mass independent mercury stable isotope fractionation. *Geochim. Cosmochim. Acta* **2011**, *75*, 4577–4590.
- (63) Yin, R. S.; Feng, X. B.; Meng, B. Stable mercury isotope variation in rice plants (*Oryza sativa* L.) from the Wanshan mercury mining district, SW China. *Environ. Sci. Technol.* **2013**, *47*, 2238–2245.
- (64) Rolison, J.; Landing, W.; Luke, W.; Cohen, M.; Salters, V. Isotopic composition of species-specific atmospheric Hg in a coastal environment. *Chem. Geol.* **2013**, *336*, 37–49.
- (65) Chen, J.; Hintelmann, H.; Dimock, B. Chromatographic pre-concentration of Hg from dilute aqueous solutions for isotopic measurement by MC-ICP-MS. *J. Anal. At. Spectrom.* **2010**, *25*, 1402–1409.
- (66) Gehrke, G. E.; Blum, J.; Meyers, P. A. The geochemical behavior and isotopic composition of Hg in a mid-Pleistocene western Mediterranean sapropel. *Geochim. Cosmochim. Acta* **2009**, *73*, 1651–1665.
- (67) Blum, J. D.; Anbar, A. D. Mercury isotopes in the late Archean Mount McRae Shale. *Geochim. Cosmochim. Acta* **2010**, *74*, A98.

(68) Zhang, H.; Yin, R.; Feng, X.; et al. Atmospheric mercury inputs in montane soils increase with elevation: evidence from mercury isotope signatures. *Sci. Rep.* **2013**, *3*, 3322.

(69) Demers, J. D.; Blum, J. D.; Zak, D. R. Mercury isotopes in a forested ecosystem: Implications for air-surface exchange dynamics and the global mercury cycle. *Global Biogeochem. Cycles* **2013**, *27*, 222–238.

(70) Han, D. X. *Coal Petrology of China*; China University of Mining and Technology Press: Xuzhou, China, 1996 (in Chinese).

(71) Yin, R. S.; Feng, X. B.; Wang, J. X.; Li, P.; Liu, J. L.; Zhang, Y.; Chen, J. B.; Zheng, L. R.; Hu, T. D. Mercury speciation, mercury isotope fractionation during ore roasting process and their implication to source identification of downstream sediment in Wanshan mercury mining area, SW China. *Chem. Geol.* **2013**, *336*, 87–95.

(72) Bouška, V.; Pešek, J.; Sykorova, I. Probable modes of occurrence of chemical elements in coal. *Acta Mont., Ser. B* **2000**, *10* (117), 53–90.

(73) Zheng, L.; Liu, G.; Chou, C.-L. Abundance and modes of occurrence of mercury in some low-sulfur coals from China. *Int. J. Coal Geol.* **2008**, *73*, 19–26.

(74) Liu, G.; Zheng, L.; Zhang, Y.; Qi, C.; Chen, Y.; Peng, Z. Distribution and mode of occurrence of As, Hg and Se and Sulfur in coal Seam 3 of the Shanxi Formation, Yanzhou Coalfield, China. *Int. J. Coal Geol.* **2007**, *71*, 371–385.

(75) Ghosh, S.; Xu, Y. F.; Humayun, M.; Odom, L. Mass-independent fractionation of mercury isotopes in the environment. *Geochem. Geophys. Geosyst.* **2008**, *9*, No. 10.1029/2007GC001827.

(76) Shi, W.; Feng, X.; Zhang, G.; Ming, L.; Yin, R.; Zhao, Z.; Wang, J. High precision measurement of mercury isotopes deposit record over the past 150 years in a peat core from Hong Yuan. *Chin. Sci. Bull.* **2011**, *56* (9), 877–882.

(77) National Bureau of Statistics. *China Energy Statistical Yearbook:2010*; China Academic Journals Electronic Publishing House: Beijing, 2011.

#### ■ NOTE ADDED AFTER ASAP PUBLICATION

This paper was originally published ASAP on May 5, 2014. There were several typos in the presentation of data in the abstract, and Hg was incorrectly written as HG twice in the body of the paper. The corrected version was reposted on May 7, 2014.